

Hot exciton transport in ZnSe quantum wells

Hui Zhao, Sebastian Moehl, Sven Wachter, and Heinz Kalt
Institut für Angewandte Physik, Universität Karlsruhe, D-76128 Karlsruhe, Germany

The in-plane transport of excitons in ZnSe quantum wells is investigated directly by microphotoluminescence in combination with a solid immersion lens. Due to the strong Fröhlich coupling, the initial kinetic energy of the excitons is well controlled by choosing the excess energy of the excitation laser. When increasing the laser excess energy, we find a general trend of increasing transport length and more importantly a pronounced periodic quenching of the transport length when the excess energy corresponds to multiples of the LO-phonon energy. Such features show the dominant role of the kinetic energy of excitons in the transport process. Together with the excitation intensity dependence of the transport length, we distinguish the phonon wind driven transport of cold excitons and defect-limited hot exciton transport.

The in-plane transport of excitons in semiconductor quantum wells (QWs) has attracted a lot of interest due to both fundamental and technological reasons. Generally, there are several possible transport processes after an optical excitation. The first one is the classical diffusion of cold excitons[1]. In this case, the excitons have the same temperature as the lattice. The transport can be well described by the diffusion equation, with a constant diffusivity. The second process is the transport of hot excitons[2], initially ballistic (before the first scattering event) and then diffusive. Since the excitons remain hot, the transport is coupled with the relaxation process. This kind of transport cannot be described by the diffusion equation, since the effective 'diffusivity' varies in both temporal and spatial domains. Beside these 'active' transport processes, which are governed by the velocity of the excitons, the excitons can also be passively driven by other factors, i.e., phonon wind[3]. Due to the increasing importance of nanostructures, transport of excitons or carriers has to be understood on a length scale comparable to the mean free path of the particles. It is obvious that here strong deviations from classical transport can be expected.

During the past two decades, the transport experiments have concentrated mainly on III-V semiconductor QWs. The employed optical techniques, namely transient-grating[4, 5], pump-probe[2, 3], time-of-flight[1, 6], microphotoluminescence (μ -PL)[7] and near-field pump-probe[8], have achieved an increasing spatial resolution. The in-plane transport of excitons in II-VI QWs was less investigated, and the transport has been regarded as classical diffusion[9, 10].

In this letter, we investigate the exciton in-plane transport in ZnSe QWs on the length scale of few μm by solid immersion lens (SIL)-enhanced μ -PL. We show that the exciton transport in this regime is not classical diffusion, but dominated by hot exciton transport. In particular, we exploit the effect that, in contrast to GaAs QWs, the initial kinetic energy of the excitons in ZnSe QWs can be tuned in a well defined manner, due to LO-phonon assisted generation of the excitons.

The confocal μ -PL system consists of a microscope

objective ($20\times$, $\text{NA}=0.4$) and a hemisphere SIL[11] of refractive index $n_r = 2.2$. The SIL is adhesively fixed to the sample surface. The spatial resolution of the whole system was determined to be about 400 nm (FWHM of the Airy pattern). The excitation source is a cw Ti:sapphire laser pumped by an Ar-ion laser and frequency-doubled using a BBO crystal. The laser beam is focused on the sample surface by the objective. The luminescence is collected by the same objective. A 20 μm pinhole in the image plane of the objective limits the detection area to 455 nm in diameter. All measurements were performed at 7 K. Two samples are studied in this investigation. Sample 1 is a 120 periods of ZnSe (7.3 nm)/Zn_{0.1}Se_{0.9} (10.7 nm) multiple QW grown by MOVPE. Sample 2 is a ZnSe (5 nm) single QW with Zn_{0.9}Mg_{0.1}Se_{0.16}Se_{0.84} barriers grown by MBE. The PL spectra of the two samples (Fig. 1) are dominated by the peaks of the heavy hole excitons (hh), with

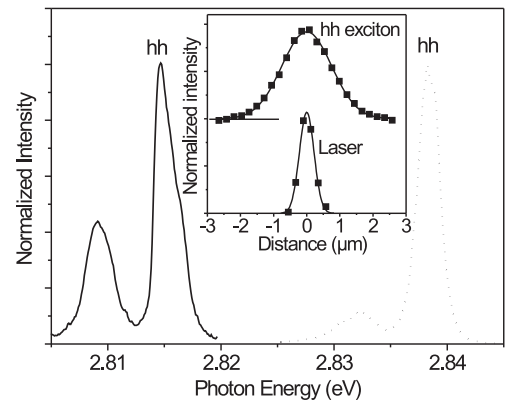


FIG. 1: Photoluminescence of sample 1 (solid) and sample 2 (dots). Inset: An example of the spatial profiles of the heavy-hole exciton luminescence (upper squares) and the laser spot (lower squares). The curves represent the corresponding Gaussian fits.

similar linewidth of about 2 meV. However, we note that the linewidth cannot be used for comparing the quality of the two samples, since the carrier confinements are different due to the different barrier materials. Actually, the luminescence efficiency of sample 2 is two orders higher than that of sample 1, that indicates the higher quality of sample 2. The samples were excited locally through the objective, and the spectra from different positions of the sample were measured by scanning the pinhole in the image plane of the objective. This allows us to gain the spatial profile of luminescence by drawing the spectrally integrated hh intensity as function of spatial position. The upper squares in the inset of Fig. 1 give an example of the spatial profiles measured in this way. By Gaussian fit, shown as the upper curve, we obtained the transport length as the FWHM of the Gaussian function. The profile of the laser spot was also measured during the same scan, as shown in the lower part of the inset.

The exciton formation and relaxation processes in these samples are well understood from monitoring the temporal evolution of the LO-phonon replica[12]. In Fig. 2, we show a schematic drawing of these processes.

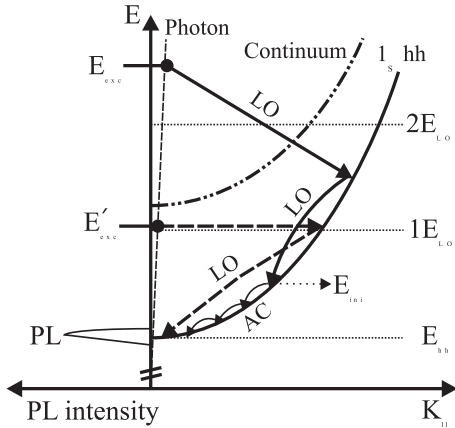


FIG. 2: Schematic drawing of the exciton formation assisted by LO-phonon emission and the subsequent relaxation by LO-phonon and acoustic phonon (AC) emissions.

After the optical excitation, the electron-hole pairs created in continuum states form excitons directly assisted by emission of LO-phonons within few ps, due to the strong Fröhlich coupling in polar II-VI quantum structures. These hot excitons relax rapidly by emission of LO-phonons, until their kinetic energy is lower than the LO-phonon energy, E_{LO} (31.8 meV for both samples, measured by Raman spectroscopy). Then the relaxation can only be achieved slowly by emission of acoustic phonons and continues over some 100 ps[12]. We define the excess energy of the excitation, E_{excess} , as the difference between the laser energy and the energy of the hh exciton resonance, $E_{laser} - E_{hh}$. In this investigation, E_{excess} is chosen such that the exciton can only emit one or two LO-phonons after formation. In this case, we can

define the exciton initial kinetic energy of the slow relaxation process realized by acoustic phonon emission to be $E_{ini} = E_{excess} - nE_{LO}$, in which n equals to 1, 2 or 3 depending on E_{excess} . By tuning the E_{excess} , we can periodically tune the E_{ini} , and thus the initial in-plane group velocity of the excitons, to investigate the influence of this velocity on the transport process.

Figure 3 shows the excess energy dependence of the transport length for both samples. When $E_{excess} < E_{LO}$, the luminescence is very weak due to the inefficient exciton formation since the LO-phonon emission path is not available. We note that in the case of $E_{excess} \approx E_{LO}$, the hh peak is superimposed by a strong resonant Raman

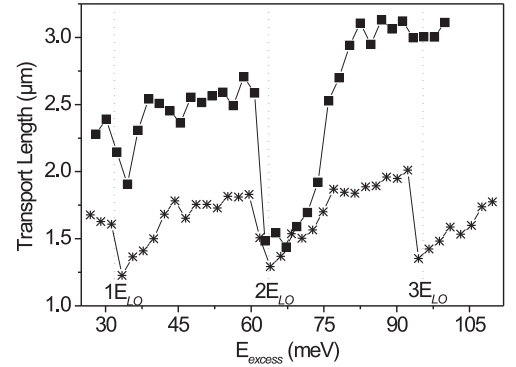


FIG. 3: Excess energy dependence of the transport length at an excitation intensity of 1 kW/cm². Sample 1: stars; sample 2: squares.

scattering peak. By multi-peak fitting, we can subtract the later from the hh peak, so the spatial profile gained in this case is not influenced by the Raman scattering. In Fig. 3, we can observe two features: (1) a general trend of increasing transport length with increasing E_{excess} and more importantly (2) a pronounced periodic quenching of the transport length when $E_{excess} \approx nE_{LO}$.

In Fig. 4, we show the excitation intensity dependence of the transport length of sample 1. Several values of E_{excess} are chosen in the range of $1E_{LO}$ to $2E_{LO}$, and the corresponding values of the E_{ini} are shown in Fig. 4. We estimate the exciton density from the excitation intensity, as shown in Fig. 4 as the top axis. An absorption coefficient of 6.5×10^4 /cm (measured by absorption spectroscopy) and a decay time of 300 ps (measured by time-resolved photoluminescence) are used for this estimation. We find from Fig. 4 that in the cases of small E_{ini} (1 meV and 7 meV), the transport length increases sub-linearly with the excitation intensity. For higher E_{ini} , the transport length is independent on the excitation intensity.

In the case of phonon wind driven transport, the transport length increases with the excitation intensity[3],

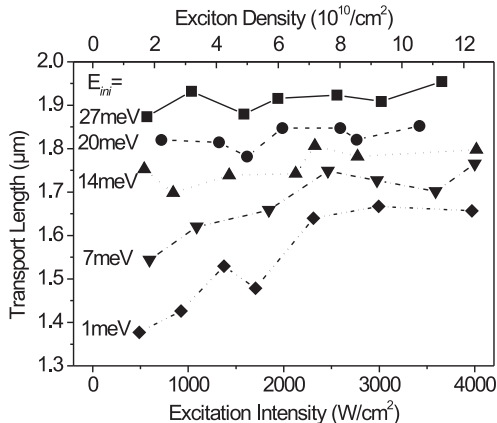


FIG. 4: Excitation intensity dependence of the transport length of sample 1.

while for the classical diffusion of cold excitons and the hot exciton transport, the transport lengths are independent on the excitation intensity. In our experiment, when the E_{excess} is slightly larger than nE_{LO} , cold excitons are generated with small E_{ini} . According to the excitation intensity dependence behavior, these cold excitons are driven by phonon wind. Increasing the E_{excess} within one period, we observe the increase of the transport length in Fig. 3. This behavior can be explained by either the hot exciton transport or the phonon wind driven model. In the former case the E_{ini} increases with E_{excess} , while in the latter case, the force of the phonon wind also increases with the E_{excess} due to the increasing of the number of phonons emitted during the relaxation of the excitons. However, the latter possibility can be ruled out by the strong periodic feature observed in Fig. 3. As mentioned above, the E_{ini} is a periodic function of the E_{excess} with a period of E_{LO} due to the fast LO-phonon emission. Thus, the periodic feature can be well explained by the hot exciton transport. In the phonon wind driven model, the wind force is anticipated to be increase monotonously with E_{excess} , since the LO-phonons emitted during the relaxation decay into acoustic phonons within few ps[13]. For these reasons, we attribute the transport of the excitons with high E_{ini} to the hot exciton transport. Actually, since the phonon wind cannot drive the excitons at drift velocities exceeding the sound velocity[3], the influence of the phonon wind on the hot excitons should be weak. The above explanations are confirmed by the independence of transport length on the excitation intensity for hot excitons, as observed in Fig. 4.

Finally, we discuss briefly the influence of defects on the transport properties. In Fig. 3, we find the transport length of sample 2 is larger than that of sample 1.

The dip around $1E_{LO}$ is more pronounced in sample 1 than in sample 2, comparing with the dips around $2E_{LO}$. In the case of $E_{excess} \approx 1E_{LO}$ (see E'_{exc} in Fig. 2), the exciton formation is inefficient due to the small momentum difference. However, the formation can be assisted by the relaxation of momentum conservation due to defects (shown as the dashed line after the E'_{exc} in Fig. 2). Thus, the dip around $1E_{LO}$ is anticipated to be more pronounced in the sample containing more defects (sample 1, due to the smaller transport length and the lower luminescence efficiency). Furthermore, the periodic feature of the transport length is more pronounced in sample 1 than in sample 2 (see the dips around $3E_{LO}$). This coincides with the fact that normally in PLE, the LO-phonon cascades are easier to be observed in the samples containing more defects, and can be attributed to the loss of excitons during the slow relaxation process. The difference of the two samples implies that the hot exciton transport in these samples is limited by defects. This statement is also consistent with calculations of the transport length from exciton acoustic-phonon interaction neglecting defects, which yields expected values of about $10 \mu\text{m}$.

In summary, we measured directly the in-plane transport of excitons in ZnSe QWs on the length scale of few μm by SIL-enhanced $\mu\text{-PL}$. Due to the strong Fröhlich coupling, the initial kinetic energy of the excitons is well controlled by tuning the laser excess energy. We find the dominant role of the kinetic energy of excitons in the transport process. The cold excitons are driven by the phonon wind. For the excitons with high initial kinetic energies, the process is dominated by the hot exciton transport. Furthermore, the hot exciton transport is limited by defects.

We gratefully acknowledge the growth of the excellent samples by the group of M. Heuken (Aachen) and the group of D. Hommel (Bremen). This work was supported by the Deutsche Forschungsgemeinschaft.

-
- [1] H. Hillmer, A. Forchel, S. Hansmann, M. Morohashi, E. Lopez, H. P. Meier, and K. Ploog, Phys. Rev. B **39**, 10901 (1989).
 - [2] H. W. Yoon, D. R. Wake, J. P. Wolfe, and H. Morkoc, Phys. Rev. B **46**, 13461 (1992).
 - [3] L. M. Smith, J. S. Preston, J. P. Wolfe, D. R. Wake, J. Klem, T. Henderson, and H. Morkoc, Phys. Rev. B **39**, 1862 (1989).
 - [4] J. Hegarty, L. Goldner, and M. D. Sturge, Phys. Rev. B **30**, 7346 (1984).
 - [5] D. Oberhauser, K.-H. Pantke, J. M. Hvam, G. Weimann, and C. Klingshirn, Phys. Rev. B **47**, 6827 (1993).
 - [6] H. Akiyama, T. Matsusue, and H. Sakaki, Phys. Rev. B **49**, 14523 (1994).
 - [7] G. D. Gilliland, M. S. Petrovic, H. P. Hjalmarson, D. J. Wolford, G. A. Northrop, T. F. Kuech, L. M. Smith, and

- J. A. Bradley, Phys. Rev. B **58**, 4728 (1998).
- [8] M. Achermann, B. A. Nechay, F. Morier-Genoud, A. Schertel, U. Siegner, and U. Keller, Phys. Rev. B **60**, 2101 (1999).
 - [9] F. P. Logue, D. T. Fewer, S. J. Hewlett, J. F. Hefferman, C. Jordan, P. Rees, J. F. Donegan, E. M. McCabe, J. Hegarty, S. Taniguchi, T. Hino, K. Nakano, *et al.*, J. Appl. Phys. **81**, 536 (1997).
 - [10] L.-L. Chao, G. S. G. III, E. Snoeks, T. Marshall, J. Petruzzello, and M. Pashley, Appl. Phys. Lett. **74**, 741 (1999).
 - [11] M. Vollmer, H. Giessen, W. Stolz, W. W. Rühle, L. Ghislain, and V. Elings, Appl. Phys. Lett. **74**, 1791 (1999).
 - [12] M. Umlauff, J. Hoffmann, H. Kalt, W. Langbein, J. M. Hvam, M. Scholl, J. Söllner, M. Heuken, B. Jobst, and D. Hommel, Phys. Rev. B **57**, 1390 (1998); H. Kalt, M. Umlauff, J. Hoffmann, W. Langbein, J. M. Hvam, M. Scholl, J. Söllner, M. Heuken, B. Jobst, and D. Hommel, J. Crystal Growth **184/185**, 795 (1998).
 - [13] S. Usher and G. P. Srivastava, Phys. Rev. B **50**, 14179 (1994), and references therein.